Am J Physiol Lung Cell Mol Physiol 290: L685–L694, 2006.
First published November 18, 2005; doi:10.1152/ajplung.00020.2005.

Contribution of proliferation and DNA damage repair to alveolar epithelial type 2 cell recovery from hyperoxia

Jooeun Lee, Raghava Reddy, Lora Barsky, Kenneth Weinberg, and Barbara Driscoll

Department of Surgery and Developmental Biology Program and Division of Research Immunology/Bone Marrow Transplant, The Saban Institute for Research, Childrens Hospital Los Angeles, University of Southern California School of Medicine, Los Angeles, California

Submitted 12 January 2005; accepted in final form 15 November 2005

Lee, Jooeun, Raghava Reddy, Lora Barsky, Kenneth Weinberg, and Barbara Driscoll. Contribution of proliferation and DNA damage repair to alveolar epithelial type 2 cell recovery from hyperoxia. *Am J Physiol Lung Cell Mol Physiol* 290: L685–L694, 2006. First published November 18, 2005; doi:10.1152/ajplung.00020.2005.—In this study, C57BL/6J mice were exposed to hyperoxia and allowed to recover in room air. The sublethal dose of hyperoxia for C57BL/6J was 48 h. Distal lung cellular isolates from treated animals were characterized as 98% epithelial, with minor fibroblast and endothelial cell contaminants. Cells were then verified as 95% pure alveolar epithelial type II cells (AEC2) by surfactant protein C (SP-C) expression. After hyperoxia exposure in vivo, fresh, uncultured AEC2 were analyzed for proliferation by cell yield, cell cycle, PCNA expression, and telomerase activity. DNA damage was assessed by TdT-dUTP nick-end labeling, whereas induction of DNA repair was evaluated by GADD-153 expression. A baseline level for proliferation and damage was observed in cells from control animals that did not alter significantly during acute hyperoxia exposure. However, a rise in these markers was observed 24 h into recovery. Over 72 h of recovery, markers for proliferation remained elevated, whereas those for DNA damage and repair peaked at 48 h and then returned back to baseline. The expression of GADD-153 followed a distinct course, rising significantly during acute exposure and peaking at 48 h recovery. These data demonstrate that in healthy, adult male C57BL/6J mice, AEC2 proliferation, damage, and repair follow separate courses during hyperoxia recovery and that both proliferation and efficient repair may be required to ensure AEC2 survival.

C57BL/6J; GADD-153; telomerase

IN LATE GESTATION OF MICE and rats, the alveolar epithelial cell (AEC) lineage develops from a multipotent population of stem cells that line the primitive respiratory tract (15). Alveolar epithelial type 2 cells (AEC2) manufacture surfactant and can differentiate, as required, into alveolar epithelial type 1 cells (AEC1), which regulate the gas exchange function of the organ (2, 14). To replace damaged cells throughout the life span of any animal, a particular subpopulation within the total population must retain the ability to divide. In the alveolar epithelium, this progenitor cell-like function has been ascribed to AEC2 (13, 31, 36). AEC2 proliferate during embryonic and fetal life but, in the adult lung, in the absence of injury, are highly differentiated and do not normally divide (9, 37). However, in response to environmental insult, some AEC2 become both hypertrophic and hyperplastic, such that cells undergo phenotypic and functional changes (17, 24). Regenerating rat AEC2 exhibit elevated cyclin and cyclin-dependent kinase (cdk) expression and activity during recovery following injury, indicating the regain of proliferative function (10, 39). During this period, the number of proliferating AEC2 has been reported to increase severalfold in rats (10, 36), mice (2), and humans (4). In human patients, this phase of recovery from lung injury has been associated with an elevated risk of morbidity and mortality (33). Hyperoxic alveolar insult induces extensive cell damage to both the vulnerable, terminally differentiated AEC1 and the differentiated portion of the AEC2 population (17). This is followed by extensive remodeling, requiring participation of the surviving AEC2 that are still capable of proliferation (8). We have recently characterized a specific subpopulation of rat AEC2 that is proliferative, expresses telomerase, and is capable of surviving hyperoxic damage, features that may allow it to orchestrate repair (12, 31).

In the mouse model, previous studies have examined the effect of hyperoxia on AEC2 in situ or as part of a whole lung homogenate, rather than on cells isolated as a pure population (22, 26–28, 30, 34, 36). To better understand the effects of hyperoxia exposure and recovery on the AEC2 isolated from one widely used laboratory animal model, we designed a series of experiments in which healthy, adult male C57BL/6J mice were systematically exposed to hyperoxia and allowed to recover in room air over set time periods. These experiments showed that a sublethal exposure time for this strain was 48 h, whereas 96 h of exposure were invariably lethal. Fresh, uncultured isolates from the lungs of these animals were characterized for homogeneity by immunohistochemical analyses and then further analyzed for markers of proliferation and DNA damage and repair. Cells exhibited a rise in both proliferation and DNA damage to levels well over baseline during the initial 24 h of recovery. In addition, while markers of proliferation remained elevated over the full 72-h recovery period, markers for DNA damage and repair peaked by 48 h and then dropped back to baseline levels. These data show that pathways for proliferation and DNA damage repair follow separate courses during recovery but may act in a coordinate fashion to restore lung epithelial equilibrium.

METHODS

Hyperoxia treatment and AEC2 culture. Male C57BL/6J mice purchased at age 6–8 wk from Jackson Laboratories (Bar Harbor, ME) were exposed to short-term hyperoxia. In brief, caged animals with food and water available ad libitum were placed in a 90 cm × 42

Address for reprint requests and other correspondence: B. Driscoll, Saban Inst. for Research, Childrens Hospital Los Angeles, MS 35, 4650 Sunset Blvd., Los Angeles, CA 90027 (e-mail: bdriscoll@chla.usc.edu).

The costs of publication of this article were defrayed in part by the payment of page charges. The article must therefore be hereby marked "*advertisement*" in accordance with 18 U.S.C. Section 1734 solely to indicate this fact.

cm × 38 cm Plexiglas chamber and exposed to humidified >95% oxygen for the times indicated. At the end of the exposure period, animals were allowed to recover in room air. Control mice were kept in room air throughout the treatment period. To isolate murine AEC2, mice were first anesthetized by intraperitoneal injection of pentobarbital. After excision of the left kidney, exsanguination was achieved via injection of sterile saline into the right ventricle of the heart with subsequent flow out through the left renal vein. Deblooded lungs were perfused in situ with dispase (GIBCO) followed by molten, 1% agarose, both in sterile saline, and both delivered via a 20-g intravenous catheter inserted into the trachea. Agarose was set by covering the chest cavity with ice for 2 min. Lungs were then removed en bloc and incubated in dispase solution with gentle agitation for 45 min at room temperature. Digested lung parenchyma was teased away from airway and connective tissue, then minced in Dulbecco's modified Eagle's medium (DMEM; Sigma, St. Louis, MO) supplemented with DNase (Sigma). The resulting cellular suspension was filtered sequentially through 100-, 70-, and 25-μm mesh to achieve a single cell suspension. Differential adherence on murine IgG-coated plates was used to eliminate white blood cell contaminants from the preparation. In brief, 100-mm Optilux dishes (Falcon, Franklin Lakes, NJ) were precoated with monoclonal antibodies CD45 and CD32/16 (Pharmingen, San Diego, CA) at 4.4 and 1.6 μg/ml, respectively, in 50 mM Tris, pH 9.5. Plates were washed thoroughly with phosphate-buffered saline (PBS) before the cellular suspension was added. Plates were incubated for 1 h at 37°C. Nonadherent cells were gently panned and recovered. Cells were pelleted at 800 *g* for 8 min and then used fresh and uncultured or suspended in DMEM with 10% FBS supplemented with antibiotics and plated at 2×10^5 cells/cm^2 in six-well plates or chamber slides coated with fibronectin (Becton-Dickinson, Bedford, MA). Cultures were maintained at 37°C in a humidified atmosphere supplemented with 5% CO_2 for the times indicated before analysis.

Immunohistochemical analysis. AEC2 cultured for 40 h in chamber slides were fixed in acetone-methanol 1:1, washed with PBS, and then blocked with CAS-Block (Zymed, San Francisco, CA). To detect cell type-specific protein expression, monoclonal antibodies to cytokeratin or vimentin (Pharmingen) were used at a concentration of 1:5,000. Purified mouse IgG (Sigma) at the same final concentration was used as the negative antibody control. Immunostaining was visualized using Alexa Fluor 555-labeled secondary antibody at 1:500 (Molecular Probes, Eugene, OR). Slides were mounted in a solution containing 4,6-diamidino-2-phenylindole for visualization of nuclei (Molecular Probes). To detect endothelial cell contaminants, an antibody to murine platelet endothelial cell adhesion molecule-1 (PECAM-1, Pharmingen) was used at 1:5,000, whereas for detection of surfactant protein (SP)-C expression, a rabbit anti-SP-C primary antibody from Chemicon (Temecula, CA) was used at 1:500 on cells fixed and blocked as described. For SP-C analysis, rabbit IgG (Sigma) at the same concentration was used as the negative antibody control. For detection of proliferating cell nuclear antigen (PCNA) expression in situ, deblooded, whole lungs were fixed in 10% formalin, then paraffin-embedded and sectioned to produce 7-μm-thick samples. Slides were deparaffinized and hydrated, then unmasked with reagent and protocol from Vector (Burlingame, CA). Slides were blocked with 5% normal rabbit serum. PCNA expression was detected using a primary monoclonal antibody from Santa Cruz Biotechnologies (Santa Cruz, CA) at a dilution of 1:200 and a Cy-3-labeled anti-mouse secondary antibody from Jackson ImmunoResearch (West Grove, PA). We used 1% bovine serum albumin (BSA) in PBS (cultured cells) or Tris-buffered saline/0.1% Tween 20 (slides) as diluents for all antibodies. Results were observed under a Leica DMA microscope at ×200.

RT-PCR for SP-C expression. Total RNA was isolated from HEL-299, rat AEC2, and murine AEC2 using the RNeasy minikit from Qiagen (Valencia, CA). The RNA yield was quantitated by UV spectrometry, and the integrity of the RNA was confirmed by analyzing for the presence of intact 28S and 18S RNA following agarose gel electrophoresis. For RT-PCR analysis, first-strand cDNA was synthesized from 2 μg of total RNA using the Omniscript-Reverse Transcriptase kit (Qiagen) to produce template cDNA, which was then used as the template for PCR amplification and analysis of specific mRNA expression. PCR was performed using reagents from the Titanium-Taq PCR kit from Clontech (Palo Alto, CA). SP-C-specific primers were designed to detect a region of the SP-C sequence with shared homology between mouse and rat. Primers mouse (m) SP-C forward (TGGTCCTTGAGATGAGCATCGG) and mSP-C reverse (GTAGAGTGGTAGCTCTCCACAC) were used to produce a 380-bp product. β-actin specific primers, actin forward (GATCTTCATGGTGCTAGGAGCC) and actin reverse (GCTCTAGACTTCGACTTCGAGCAGGAGA), were used to produce a 367-bp product.

Western blotting for PCNA and GADD-153. Fresh, uncultured AEC2, isolated from control and hyperoxia-treated animals, were lysed by incubation in radioimmunoprecipitation assay buffer for 30 min on ice. Insoluble material was pelleted by centrifugation at 13,000 *g* for 10 min. Total soluble cellular protein was then analyzed for PCNA and GADD-153 expression by Western blotting. Mouse monoclonal antibody to PCNA was obtained from Santa Cruz Biotechnologies, whereas rabbit polyclonal antibody to GADD-153 was from AbCam (Cambridge, MA). Both were used at a concentration of 1 μg/ml. Horseradish peroxidase-labeled goat anti mouse IgG and goat anti-rabbit IgG from Sigma were used as secondary antibodies at 1:25,000. Specific antibody binding was visualized using ECL reagents from Amersham to detect chemiluminescence. To analyze differences in protein expression between control samples, specific bands from three separate blotting experiments were subjected to densitometric scanning and normalization to actin. Analysis was performed on a Macintosh computer using the public domain NIH Image program (developed at the U.S. National Institutes of Health and available on the internet at http://rsb.info.nih.gov/nih-image/).

Fluorescence-activated cell sorting analysis for proliferative profile and TdT-dUTP nick-end labeling. Fresh, uncultured AEC2 were fixed with 1% paraformaldehyde in PBS for 15 min on ice. After being washed, cells were incubated in 70% ethanol at −20°C for at least 24 h before TdT-mediated dUTP nick end labeling (TUNEL) analysis was performed according to the Apo-Direct kit manufacturer's instructions (PharMingen). In brief, fixed cells were washed and then incubated with TdT enzyme and substrate (FITC-dUTP) for 1 h at 37°C. After being washed, cells were counterstained with a propidium iodide-RNase solution. Samples were analyzed using a Becton Dickinson FACScan and CellQuest software. Parameters for TUNEL were set with positive and negative control cells supplied with the Apo-Direct kit. For these experiments, 10,000 events were acquired, and the nonclumped cells were gated for analysis. These data sets were used to both analyze cell cycle profile of the entire gated sample and to calculate the percentage of the total that were TUNEL positive. Events were analyzed for DNA content and cell cycle phase percentages using ModFit LT version 2.0 DNA analysis software (Verity Software House, Topsham, ME). For detection of TUNEL in situ, slides were prepared as described for immunohistochemistry with the exception that antigen unmasking was not performed. Samples were subjected to TdT nick end labeling using reagents from the Apo-Direct kit.

Telomerase repeat amplification protocol assay. Sample preparation and telomerase repeat amplification protocol (TRAP) assays were performed according to the TRAP-EZE protocol (Chemicon, Temecula, CA). Briefly, at least 10^6 fresh, uncultured AEC2 from each indicated time point were lysed in 1× CHAPS lysis buffer. The lysate was clarified by centrifugation, and protein content was measured. To assess telomerase activity, we incubated samples containing 50 ng of protein with a [γ-^{32}P]dATP end-labeled telomerase-specific primer at 30°C for 30 min for telomere primer extension. The telomerase products were amplified by 30 rounds of two-step PCR (94°C/30 s, 60°C/30 s). The samples were subjected to 12.5% nondenaturing

polyacrylamide gel electrophoresis (PAGE) in 0.5× TBE buffer (45 mM Tris-borate, 1 mM EDTA) for 1 h at 500 V. Gels were dried and exposed to X-ray film to visualize the telomerase products. Each assay included a positive control and a PCR contamination control lane consisting of all sample elements with the exception of cell lysate. Before each analysis, all cell samples were individually analyzed for nonspecific PCR products by heating at 85°C for 10 min to inactivate telomerase. Any samples exhibiting nonspecific products by TRAP were not used for experiments.

Statistics. Data were analyzed by Tukey's test for multiple comparison of means and are given as means ± SE.

RESULTS

The majority of distal lung cells isolated from C57BL/6J mice express the epithelial cell-specific marker cytokeratin. Murine AEC2 were isolated by an adaptation of methods previously described by Corti et al. (11) and Rice et al. (32). Yield per 6- to 8-wk-old mouse was routinely 3 million to 5 million cells. These protocols use antibodies to hematopoietic markers in a differential plating scheme during isolation to eliminate blood cell contaminants. Antibodies to the CD45 antigen, which is expressed on all murine cells of hematopoietic origin except for erythrocytes and platelets, and the CD32/16 antigen, which is specific for mouse macrophages, were used to immobilize monocytes and leukocytes and remove them from the crude lung isolate. By fluorescence-activated cell sorting (FACS), the majority of mouse lung cells obtained by the methods described are large and granular, falling within gates previously established for rat AEC2 (7, 8).

To determine the identity of these cells, we fixed cultured isolates and then immunostained them to detect expression of cytokeratin, considered an epithelial cell-specific marker, or vimentin, considered a marker specific for fibroblasts (20). According to these differential expression markers, the majority of cells obtained were of epithelial origin (Fig. 1). By a count of multiple fields under microscopy, 97.6 ± 2.1% were cytokeratin positive. In contrast, vimentin-positive contaminants were rarely observed (1.8 ± 0.6%) (n = 7 isolations). Rare endothelial cell contaminants, characterized by PECAM-1 expression, were observed too infrequently to be considered a significant contaminant. From these data, we conclude that fibroblast and endothelial cell contamination of murine lung epithelial cell isolates is minimal.

A significant majority of cells isolated from murine distal lung are AEC2, as determined by SP-C expression. After ~40 h in culture, lung epithelial cells were fixed with acetone-methanol and immunostained to detect expression of the AEC2-specific marker, SP-C. Rabbit IgG was used as a negative control for expression. For multiple isolations, SP-C-positive AEC2 were estimated to routinely compose 93–95% of all cells. Although somewhat morphologically distinct from rat AEC2, which exhibit a rounded, cobblestone shape, the majority of the more triangular murine AEC2 exhibited high levels of SP-C expression by immunostaining (Fig. 2*A*). The level of SP-C mRNA expression in murine AEC2 was also similar to that of rat AEC2 (Fig. 2*B*). mRNA extracted from 24-h cultures (D1) of murine and rat AEC2 were analyzed for SP-C mRNA by RT-PCR. The SP-C-null cell HEL-299, an immortalized human pulmonary fibroblast line, was used as a negative control for surfactant expression. Primers for RT-PCR were specific for murine SP-C but were chosen to correspond to a region of mouse/rat homology, enabling amplification of rat SP-C. Expression of β-actin mRNA was used as an internal control. Together, data presented in Figs. 1 and 2 show that the method used to isolate AEC2 from murine distal lung produces a relatively homogenous population of AEC2.

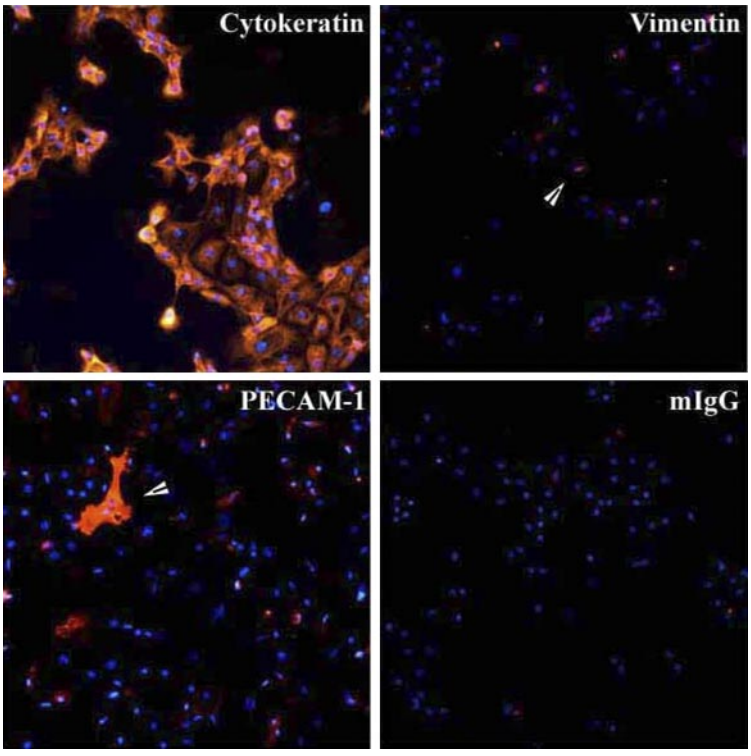

Fig. 1. The majority of cells isolated from C57BL/6J distal lung express the epithelial cell-specific marker cytokeratin. Murine distal lung cells were isolated from mice by an adaptation of methods previously described (11, 32). Cells were plated on fibronectin-coated plates for culture in DMEM supplemented with 10% FBS. After fixation in acetone-methanol (1:1), 48-h cultures were immunostained to detect expression of cytokeratin, vimentin, or platelet endothelial cell adhesion molecule (PECAM)-1. An Alexa Fluor 555-labeled secondary antibody was used to detect signal. The majority of cells isolated by this method were cytokeratin positive. Vimentin-positive fibroblast contaminants and PECAM-1-positive endothelial cell contaminants were rarely observed (arrowheads). Mouse IgG (mIgG) at a concentration identical to specific primary antibodies was used as a negative control for staining.

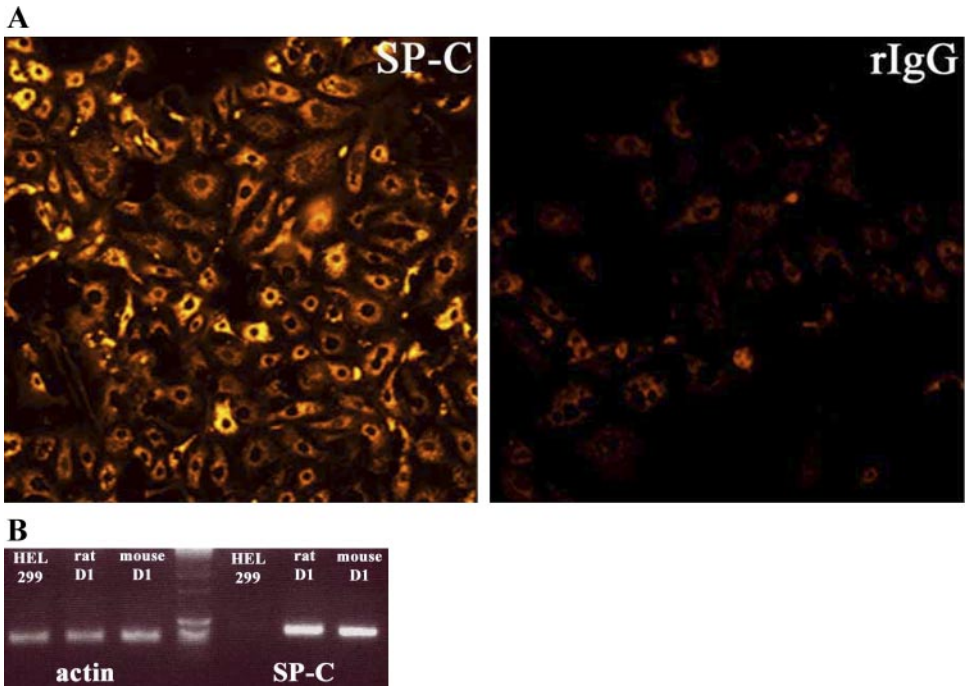

Fig. 2. A significant majority of cells isolated from murine distal lung are surfactant protein (SP)-C positive. *A*: acetone-methanol-fixed lung epithelial cells were immunostained to detect expression of SP-C using a specific primary antibody from Chemicon. Positive expression was visualized using an Alexa Fluor 555-labeled secondary antibody. Rabbit IgG (rIgG, *right*) was used as a negative control. *B*: mRNA extracted from 24-h cultures (D1) of mouse AEC2 was analyzed for SP-C mRNA by RT-PCR, which produced a 380-bp band. Expression in murine AEC2 was comparable to D1 cultures of adult rat alveolar epithelial type II cells (AEC2). SP-C-null HEL299 was used as a negative control. Expression of a 367-bp β-actin product was used as an internal control. (The central lane containing multiple bands is a molecular weight marker.)

The sublethal dose of hyperoxia for C57BL/6J mice is 48 h. To determine the effect of a sublethal dose of hyperoxia on murine AEC2 function and survival, a model for exposure of C57BL/6J mice was developed. Animals exposed to >95% inspired oxygen for designated periods within a 96-h time frame and then allowed to recover in room air for designated periods within a 72-h time frame were monitored twice daily for signs of distress leading to death. Data for survival of exposure and recovery are presented in Fig. 3, in which the 100% survival rate of control animals that breathed room air was compared with those exposed for 24, 48, 72, and 96 h. Mice exposed for 24 h showed no ill effects, either during exposure or during recovery in room air. Acute exposure for 48 h was survivable for all animals examined ($n = 17$), though some succumbed during recovery. The survival rate at 24 h of recovery was 88.89 ± 5.67% ($n = 17$), which rose to 93.75 ± 8.33% ($n = 14$) by 72-h recovery. Though this change showed an intriguing trend, in that animals that did not succumb by 24 h following exposure were more likely to survive as recovery progressed, this increase in survival rate over time was not statistically significant. A slight majority of animals exposed for 72 h also survived (61 ± 8.84%, $n = 11$). However, many more of these mice died during recovery, with only 58.33 ± 12.2% ($n = 6$) surviving 24 h in room air, dropping to 29.25 ± 11.04% ($n = 13$) surviving for 72 h after hyperoxia exposure. Without exception, 96 h of exposure resulted in death ($n = 4$). From these data we concluded that a sublethal acute exposure time for healthy, adult male C57BL/6J mice was 48 h.

Acute exposure to hyperoxia does not stimulate murine AEC2 proliferation, but a strong induction of proliferation is observed during recovery. To determine the effect of hyperoxia exposure and recovery on distal lung epithelial cells, fresh, uncultured AEC2 from animals treated over the sublethal time course previously described were analyzed for markers of proliferation. Because we wished to determine the status of AEC2 immediately following treatment without the influence of culture, fresh isolates only were examined. However, aliquots of cells isolated from treated animals were routinely plated and examined for the presence of contaminating cells by immunohistochemistry. These analyses showed that populations isolated from hyperoxia-exposed and recovering animals were homogenous AEC2 containing an extremely low number of fibroblast and endothelial cell contaminants, as was previ-

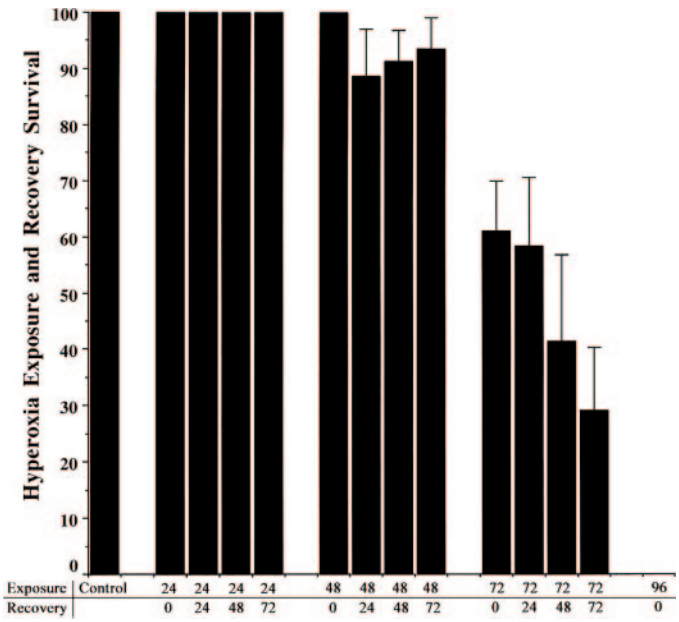

Fig. 3. A sublethal dose of hyperoxia and a time frame for recovery were determined for C57BL/6J mice. Exposure of 6- to 8-wk-old C57BL/6J mice to >95% inspired oxygen showed the sublethal exposure time frame extends to 48 h. Time points examined: control animals that breathed room air, 24, 48, and 72 h exposure with 0, 24, 48, and 72 h recovery in room air and 96 h exposure.

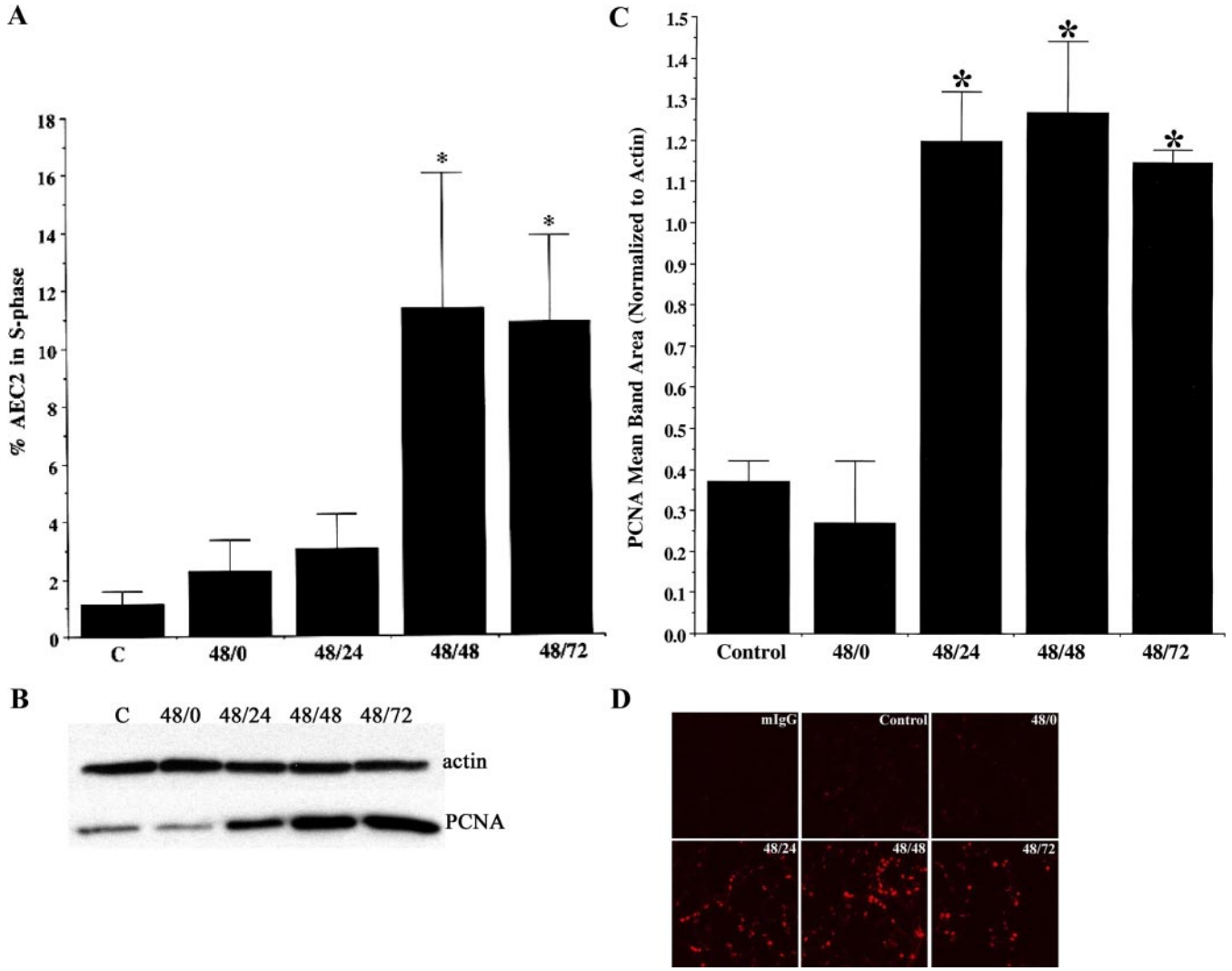

Fig. 4. AEC2 isolated from animals recovering from hyperoxia are proliferative compared with cells from control mice. *A*: percentage of AEC2 in S-phase was significantly elevated in animals recovering from hyperoxia compared with AEC2 isolated from control mice. Fresh, uncultured AEC2 were fixed and stained with propidium iodide to determine DNA content. Cell cycle analysis of cells was performed by a FACS assay followed by ModFit analysis. The mean percentage of cells in S-phase were: in controls, 1.12 ± 0.44%; at 48-h exposure/0-h recovery, 2.28 ± 1.07%; at 48-h exposure/24-h recovery, 3.05 ± 1.19%; at 48-h exposure/48-h recovery, 11.36 ± 4.71%; and at 48-h exposure/72-h recovery, 10.87 ± 2.99%. (For all time points, given in hours, $n = 3–6$; all values are means ± SE.) Data were analyzed by Tukey's test for multiple comparison of means, which showed that values for the 48/48 and 48/72 time points were significantly different from control, 48/0, and 48/24 values, $^*P < 0.05$. *B*: Western blotting showed sustained, upregulated expression of PCNA in AEC2 from animals recovering from hyperoxia. Fresh, uncultured AEC2 were analyzed for changes in PCNA, a marker for cellular proliferation. Animals were exposed to hyperoxia for 48 h, then allowed 0–72 h to recover. Blotting for β-actin expression was used as a loading control. *C*: densitometric scanning of multiple PCNA blotting experiments showed that the upregulation of PCNA expression during recovery was statistically significant. Densitometric scanning for band area values was performed on blots from 4 separate experiments. Results were expressed as the ratio of PCNA/actin expression and means obtained for each treatment period. Data were analyzed by Tukey's test for multiple comparison of means, which showed that values for the 48/24, 48/48, and 48/72 time points were significantly different from the control value, $P < 0.05$. *D*: analysis of PCNA expression in lung tissue in situ showed that changes in expression levels paralleled those observed in fresh, uncultured AEC2. Formalin-fixed, paraffin-embedded tissue sections of lungs harvested from control, hyperoxia-exposed, and recovering animals were subjected to immunohistochemical analysis for PCNA expression. Cells positive for PCNA were detected using an anti-PCNA primary antibody and a Cy-3-labeled secondary antibody. mIgG was used as a negative control.

ously observed for isolates from control animals. Analysis of the DNA content of fresh, uncultured AEC2 showed that proliferation, as indicated by activation of the cell cycle, was strongly induced during the recovery phase. A significant increase in the proportion of total AEC2 in S-phase was observed in the first 24 h of recovery (Fig. 4*A*). By this marker, proliferation peaked significantly by 48 h and remained elevated at 72 h. (For all time points, $n = 3–5$.) These data were supported by Western blotting for expression of PCNA in AEC2 from control, hyperoxia-exposed, and recovering animals (Fig. 4*B*). Expression of PCNA, which, together with p53, regulates DNA replication and repair and is a standard marker for cellular proliferation, was significantly altered by these treatments. The negligible levels of PCNA expression in murine AEC2 at baseline remain essentially static during exposure to hyperoxia. However, strong induction of expression was routinely observed when animals were allowed to recover in room air. Blotting for β-actin expression was used as a loading

control. These data were quantified by densitometric scanning, and results are shown in Fig. 4*C*. These data show that the rise in PCNA expression at 24, 48, and 72 h of recovery compared with control or acute exposure samples was highly statistically significant by Tukey's test ($*P < 0.05$). This rebound in PCNA expression, significantly elevated by 24 h of recovery, correlated with the rise in the number of AEC2 and the proportion of those cells in S-phase at that same time point. In an effort to quantitate this observation, we graphed the mean number of cells in S-phase against the mean level of PCNA expression for each time point. These numbers were obtained from each assay as presented in Fig. 4, *A* and *C*. Using a simple curve fit, we found a strong positive correlation between changes in the number of cells in S-phase and changes in PCNA expression, with the value of the coefficient of determination approaching 1 ($R^2 = 0.895$). These data reflect observations made on whole lung sections from control, hyperoxia-treated, and recovering animals, where immunohistochemical analysis showed that low, baseline PCNA expression increased considerably during the recovery period (Fig. 4*D*).

Elevated levels of PCNA and an increase in the number of cells in S-phase do not result in a significant increase in the numbers of AEC2 isolated from recovering animals. Quantitated data presented in Fig. 4 were obtained from freshly isolated samples, which were assumed to reflect changes in proliferation markers in vivo. This assumption was confirmed by analysis of changes in PCNA expression in whole lung sections. By this marker, AEC2 proliferation dramatically increases during recovery following exposure to hyperoxia. However, this change in proliferative profile did not result in a significant alteration of cell number. As shown in Fig. 5, fresh, uncultured AEC2 were analyzed for numbers of viable cells recovered by Trypan blue exclusion and examination by microscopy. A total of $4.3 \pm 0.37 \times 10^6$ cells was recovered from control animals that breathed room air ($n = 15$). This number did not change significantly when cells were isolated from animals exposed to hyperoxia for 48 h, where the mean number of cells isolated was $4.0 \pm 0.17 \times 10^6$ ($n = 9$). Numbers of cells isolated increased as animals recovered from hyperoxia, with a mean $4.6 \pm 0.94 \times 10^6$ ($n = 7$) cells isolated at 24 h of recovery, peaking at $5.6 \pm 0.45 \times 10^6$ ($n = 7$) cells at 48 h of recovery. At 72-h recovery, the mean number of cells isolated was $5.2 \pm 0.54 \times 10^6$ ($n = 7$). Though these increases in cell number during recovery were routinely observed, they were not significantly different from values obtained from control or acutely treated animals by Tukey's test for comparison of multiple means.

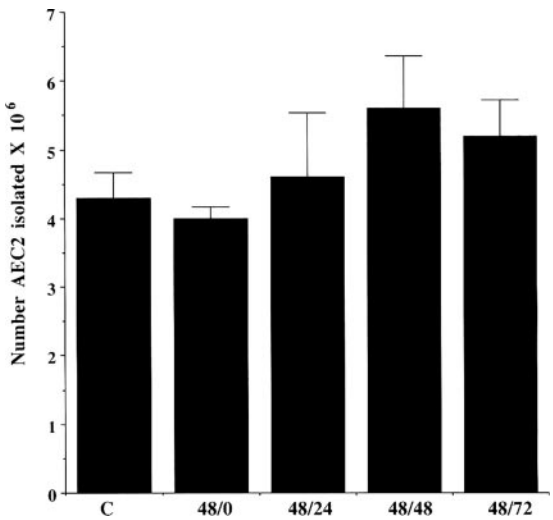

Fig. 5. The number of cells isolated from recovering animals is routinely, though not significantly, greater than the number isolated from controls. Fresh, uncultured AEC2 were analyzed for numbers of viable cells recovered using Trypan blue exclusion and examination by microscopy. A mean 4.3×10^6 cells could be recovered from control animals ($\pm 0.37 \times 10^6$, $n = 15$). Acute exposure to hyperoxia for 48 h yielded $4.0 \pm 0.17 \times 10^6$ cells ($n = 9$). During recovery from hyperoxia, mean yields were, at 48/24: $4.6 \pm 0.94 \times 10^6$ cells ($n = 7$), at 48/48: $5.6 \pm 0.45 \times 10^6$ cells ($n = 7$), at 48/72: $5.2 \pm 0.54 \times 10^6$ cells ($n = 7$). Though the rise in cell number during recovery was routinely observed, the increase over numbers obtained from control isolates was not statistically significant by Tukey's test for multiple comparison of means.

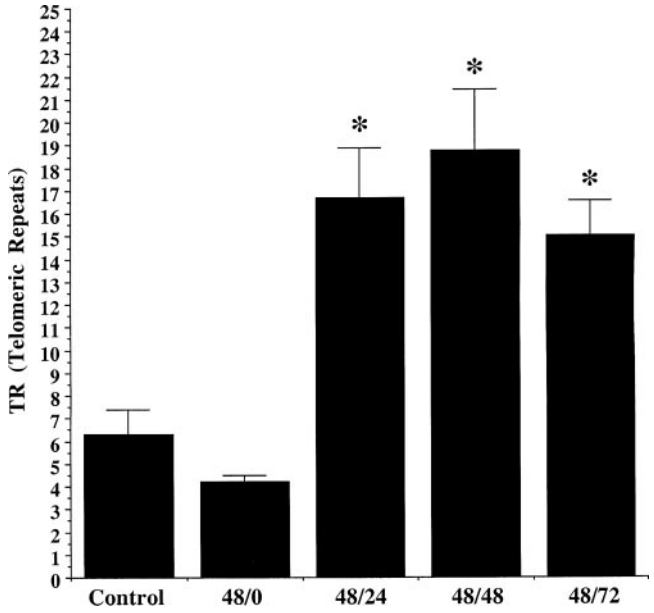

Fig. 6. Telomerase activity in murine AEC2 is upregulated during recovery from hyperoxia. Fresh, uncultured AEC2 from mice exposed to hyperoxia and allowed to recover for the time indicated were analyzed for telomerase activity by telomerase repeat amplification protocol (TRAP). (For each time point, $n = 3$.) For control, telomerase repeat (TR) was 6.3 ± 1.1, while 48/0 TR was 4.2 ± 1.3. The TR at 24-h recovery rose to 16.7 ± 2.2. TR at 48-h recovery was 18.8 ± 2.7 and 15.1 ± 1.5 by 72 h. Values for mean TR were all significantly different from values for both control and the 48/0 time points as analyzed by Tukey's test, $*P < 0.05$.

Telomerase activity in murine AEC2 is upregulated during recovery from hyperoxia. We have previously observed that upregulation of telomerase activity occurs in AEC2 isolated from hyperoxia-exposed rats (12). To determine whether enzyme activity is also induced in murine AEC2, fresh, uncultured cells from mice exposed to hyperoxia and allowed to recover for the times indicated were analyzed by TRAP. To obtain quantifiable data, we counted the number of telomerase repeats (TR) generated by individual samples for each time point. As shown in Fig. 6, a measurable, though moderate, baseline level of telomerase activity was observed in AEC2 from control animals, similar to the level we have observed in rat AEC2 (12). This activity dropped slightly, though not significantly, during 48 h exposure to hyperoxia. However, as animals recovered, telomerase activity rose significantly over baseline and remained elevated over the 72 h of recovery

analyzed. Statistical analysis of data from four separate experiments showed that for AEC2 from control mice, the mean TR was 6.3 ± 1.1. The mean TR during acute exposure dropped to 4.2 ± 1.3. At 24-h recovery, the mean TR rose to 16.7 ± 2.2, while mean TR at 48-h recovery was 18.8 ± 2.7. These numbers paralleled the TR routinely observed in rat AEC2 isolated from hyperoxia-exposed and recovering animals. By 72 h of recovery, the mean TR was 15.1 ± 1.5 still significantly elevated over control, as were TR at 24 and 48 h of recovery (all $*P < 0.05$). These data parallel the observed rise in the proportion of cells in S-phase and the increase in PCNA expression observed in murine AEC2 in vivo, confirming that proliferation remains elevated during the recovery period. As telomerase is also considered a marker for DNA repair (16), we then proceeded to determine the level of DNA damage in AEC2 from hyperoxia-exposed and recovering mice.

AEC2 from C57BL/6J mice recovering from sublethal hyperoxia exposure exhibit an elevated level of DNA damage 24 h into recovery, which drops to control level by 72 h. TUNEL analysis of murine AEC2 isolated from animals exposed to a sublethal dose of hyperoxia was performed to determine the level of DNA damage incurred by exposure (for each time point, $n = 3–6$). The resulting data are shown in Fig. 7*A*. Fresh, uncultured AEC2 isolated from control animals showed a measurable (though minimal) level of TUNEL at a mean of 2.29 ± 1.71% positive cells. The number of TUNEL-positive cells decreased during 48 h of acute hyperoxia exposure, though this drop was not significant. However, as animals recovered in room air for 24–48 h, the observed level of DNA damage rose sharply. TUNEL for both time points was significantly elevated over control, though a slight decrease at 48-h recovery could already be observed. At 24 h of recovery, the mean percentage of TUNEL-positive cells was 84.09 ± 11.67%, a significant increase compared with controls ($*P < 0.05$). At 48 h of recovery, the mean percentage of TUNEL-positive cells had dropped to 55.56 ± 23.81%, though this number also reflected a significant degree of damage ($*P < 0.05$). By 72 h, TUNEL levels had dropped to a mean of 6.54 ± 4.15%, not significantly different from control, but significantly different from levels at 24 and 48 h of recovery. These data indicate a notable increase in AEC2 DNA damage over baseline in vivo early in the recovery period, which dropped as recovery proceeded, findings that parallel observations made from a similar TUNEL analysis on whole lung sections (Fig. 7*B*). Thus, while AEC2 were presumably damaged at the level of single- and double-strand nicking by hyperoxia exposure, DNA integrity was eventually restored during recovery. We noted that AEC2 proliferation remained elevated during this same period (Fig. 4) and speculated that ongoing DNA repair, which can also be detected as a positive TUNEL signal, may take a separate path from the mechanism driving proliferation in this same population.

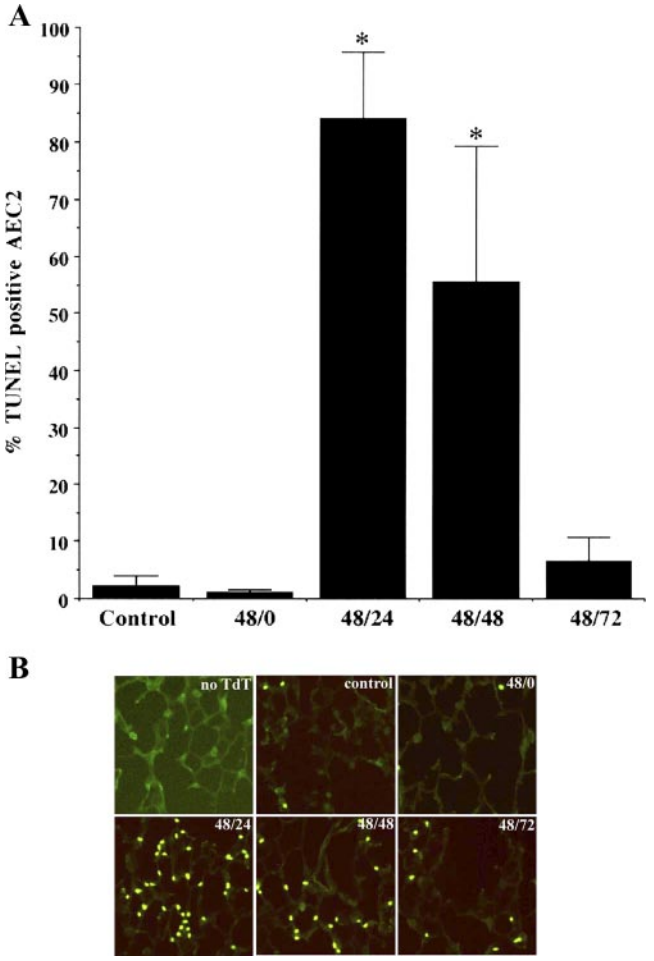

Fig. 7. *A*: TdT-mediated dUTP nick end labeling (TUNEL) analysis of murine AEC2 from hyperoxia-exposed animals shows an elevated level of DNA damage early in recovery that quickly resolves. Fresh, uncultured AEC2 were fixed and analyzed for DNA damage by TUNEL. (For each time point, $n = 3–6$.) In control animals, the percentage of TUNEL-positive cells was 2.29 ± 1.71%. During exposure to hyperoxia, the mean was 1.13 ± 0.45%. As animals recovered for 24–48 h, the level of DNA damaged was significantly elevated over control (48/24, 84.09 ± 11.67%; 48/48, 55.56 ± 23.81%). By 72-h recovery, TUNEL-positive AEC2 were a mean 6.54 ± 4.15%. By Tukey's multiple-comparison test, values for control and 48/0 differed significantly from values for 48/24 and 48/48 ($*P < 0.05$), but not from the value for 48/72. *B*: TUNEL analysis in situ of lung tissue sections revealed a pattern of DNA damage similar to that observed in isolated AEC2. Lungs from control, hyperoxia-treated, and recovering animals were fixed and paraffin-embedded and then sectioned for in situ analysis. To control for background fluorescence, a sample including FITC-dUTP but no TdT enzyme was used as a control.

Expression of the DNA repair enzyme GADD-153 is upregulated in murine AEC2 upon exposure to hyperoxia and during the early phase of recovery. To determine whether the resolution of DNA damage observed in cells isolated from animals recovering from hyperoxia could be due to upregulated repair, the expression level of the DNA repair enzyme GADD-153 was determined by Western blotting (Fig. 8*A*). In agreement with published reports that showed hyperoxia-induced upregulation of GADD-153 in mouse lung in vivo (27), GADD-153 expression in fresh, uncultured AEC2 began to increase upon 48 h of acute exposure to hyperoxia and peaked at 48 h of recovery. Unlike PCNA expression, cell number, and telomerase activity, which remained elevated through 72-h recovery, GADD-153 expression decreased by that point, perhaps indicating a difference in pathways regulating proliferation and repair during recovery. (Note that samples used for the example in Fig. 8*A* are identical to those used to determine PCNA expression in Fig. 4*B*, and as such, an identical actin blot is used to demonstrate equal protein loading.) Quantitation of GADD-153 expression from multiple sets of hyperoxia exposure and recovery experiments is shown in Fig. 8*B* ($n = 3$).

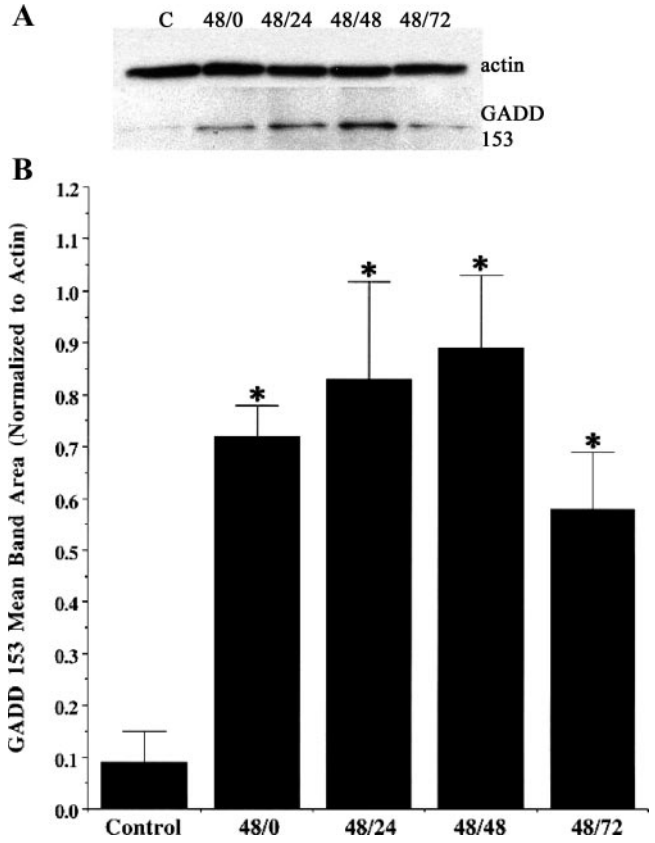

Fig. 8. *A*: expression of the DNA repair enzyme GADD-153 is upregulated in murine AEC2 upon exposure to hyperoxia and during the early phase of recovery. The expression levels of the DNA repair enzyme GADD-153 were determined by Western blotting. GADD-153 expression in fresh, uncultured AEC2 was elevated upon 48-h exposure to hyperoxia, peaked at 48 h of recovery, and then decreased by 72 h. (Note that samples used for the example in Fig. 7*A* are identical to those used to determine PCNA expression in Fig. 4*B*, and as such, an identical actin blot is used to demonstrate equal protein loading.) *B*: densitometric scanning of multiple GADD-153 blotting experiments showed that the upregulation of repair enzyme expression during hyperoxia exposure and recovery was statistically significant. Densitometric scanning for band area values was performed on blots from 3 separate experiments. Values were normalized to parallel blots for actin and means obtained for each treatment period. Multiple-comparison analysis (Tukey's test) showed mean values for all time points (48/0, 48/24, 48/48, and 48/72) were significantly different from control mean value ($*P < 0.05$).

Densitometric scanning of blots revealed that the elevation in expression at all time points following 48-h hyperoxia exposure was significant over control ($*P < 0.05$). With arbitrary values normalized to actin expression for each sample, the level of GADD-153 expression at 48 h of exposure to oxygen with no recovery rose sharply to a mean of 0.72 ± 0.06 vs. 0.09 ± 0.06 for control. These levels were further elevated during the early period of recovery, to a mean of 0.83 ± 0.19 at 24 h and 0.89 ± 0.14 at 48 h of recovery. GADD-153 expression levels dropped to a mean of 0.58 ± 0.11 by 72-h recovery, though this value was still significantly elevated compared with control levels.

DISCUSSION

The C57BL/6J mouse strain is a valuable model for lung injury and repair studies, not least because it is the foundation stock for a number of useful transgenic strains. We note that healthy, adult male C57BL/6J mice are slightly more resistant to hyperoxia exposure than adult male Sprague-Dawley rats and that the effects of hyperoxia we observe are similar to the findings of Hudak and colleagues (18), who predicted the response of several mouse strains to distal lung inhalant injury based on differences in alveolar structure. We speculate that similar results would be obtained in healthy adult female C57BL/6J mice and would be most interested in examining the process of recovery in newborns, which are more resistant to acute hyperoxia exposure than adult animals. We also found that adherent cells cultured from distal lungs of C57BL/6J mice are a surprisingly homogeneous population, almost uniformly cytokeratin positive, as seen in Fig. 1. Further characterization showed that the majority of the epithelial cells isolated express SP-C, thus demonstrating that the methods adapted from Corti et al. (11) and Rice et al. (32) can be successfully used to produce useful numbers of pure murine AEC2.

For further studies, we elected to use fresh, rather than cultured, isolates. We wished to determine the effects of hyperoxia and recovery on murine AEC2 as they exist in vivo, without the influence of culture on fibronectin, which has been shown to have a significant effect on the proliferation and survival of AEC2 isolated from hyperoxia-treated rats (8). By comparing results for some parameters from fresh, uncultured AEC2 with those obtained by examining whole lung tissue sections, we showed that data quantified from purified AEC2 paralleled observations made on whole lung in vivo. In situ changes, specifically in PCNA expression (Fig. 4) and DNA damage as measured by TUNEL (Fig. 7), though they could not definitively be assigned to AEC2, nevertheless verified that results from purified isolates reflected the status of those cells in vivo in response to hyperoxia treatment and recovery.

Using the purified isolates, we were able to determine that AEC2 from mice in the acute phase of sublethal exposure, like those isolated from control animals, are quiescent and appear undamaged at the level of DNA strand nicks. This suppressive effect of hyperoxia exposure in vivo has been widely noted (21, 26, 35, reviewed in 28). Once animals were moved back to room air to recover, significant changes in markers for proliferation, damage, and repair occurred. Cells appeared to become markedly proliferative, with increases in the number of cells in S-phase, the level of PCNA expression, and the induction of telomerase activity all significant as early as 24 h into recovery. This observation could be due an S-phase, cell-cycle block, which could account for the relative stability of cell numbers isolated from treated and recovering animals at all time points. However, we also note that markers for proliferation remained elevated over 72 h, an extensive period for cells that appear to be responding quite dynamically to the hyperoxic insult. In contrast, while the number of AEC2 exhibiting DNA strand nicks by TUNEL also rose during recovery, the number of damaged cells dropped precipitously by 72 h, back to levels not significantly different from controls. Preceding this phenomenon was the rise in expression of the DNA repair enzyme GADD-153, which first appeared during acute exposure, indicating that activation of repair pathways, which can also induce a positive TUNEL signal, could account for the subsequent drop off in damage. We note with interest that while the actual number of AEC2 isolated from recovering animals is greater than the number obtained from control animals, this difference is not significant. It may be that the

induction of proliferation, damage, and repair during recovery from hyperoxia results in a dynamic interaction between pathways that act together to maintain a required level of viable AEC2 within the distal lung.

It is theorized that oxidative stress effects are mediated by both accumulation of inflammatory factors and direct effects of reactive oxygen species (ROS) (3, 19, reviewed in 29). Multiple changes in whole lung gene expression can be observed by microarray even after short-term exposure to hyperoxia, indicating that multiple cellular pathways may play a role in cellular response (30). Other studies at the whole lung level show that activation of the c-Jun NH_2-terminal kinase (JNK) pathway may confer a certain level of protection from hyperoxia, as *jnk*−/− mice are significantly more susceptible to its lethal effects (25). DNA repair pathways that require normal function of p53, the cdk inhibitor p21, and the DNA damage response genes GADD-45 and GADD-153 all play major roles in the murine response to hyperoxic insult, specifically at the level of AEC2 (22, 23, 26, 27, 35, 38, reviewed in 28). These data also support the observation that one of the targets of ROS is AEC2 DNA, as evidenced by the appearance of 8-hydroxy-2′-deoxyguanosine, a product of DNA oxidation, in murine AEC2 from hyperoxia-exposed animals (34). However, the pathways activated in response to release from this checkpoint have so far not been thoroughly examined.

Our data show that while proliferation during recovery from sublethal hyperoxia exposure may occur and may be required to replace terminally damaged cells, the induction of repair mechanisms may also strongly influence the ability of the distal lung to return to equilibrium. At this time we cannot determine which of these pathways is the dominant mechanism for maintenance, or whether a coordinate effort is required. Seventy-two hours into recovery, markers for proliferation were still elevated over baseline but were noticeably dropping. We therefore speculate that analysis over a longer recovery period would not show a significant increase in cell number and that, in this model of hyperoxia injury and recovery, the drive toward equilibrium is strong.

ACKNOWLEDGMENTS

The authors thank Dr. Fred Dorey and Made Wenten in the Statistics Core of Childrens Hospital Los Angeles for help in data analysis. We also thank Prasadarao Nemani for critical reading of this manuscript.

GRANTS

This work was supported in part by National Heart, Lung, and Blood Institute Grants R01 HL-65352 to B. Driscoll and NIH R21 HL-72211 to C. Lutzko (principal investigator).

REFERENCES

1. **Adamson IY, Bowden DH, and Wyatt JP.** Oxygen poisoning in mice. Ultrastructural and surfactant studies during exposure and recovery. *Arch Pathol* 90: 463–472, 1970.
2. **Adamson YR and Bowden DH.** The type 2 cell as progenitor of alveolar epithelial regeneration. A cytodynamic study in mice after exposure to oxygen. *Lab Invest* 30: 35–42, 1974.
3. **Auten RL, Whorton MH, and Nicholas Mason S.** Blocking neutrophil influx reduces DNA damage in hyperoxia-exposed newborn rat lung. *Am J Respir Cell Mol Biol* 26: 391–397, 2002.
4. **Bachofen M and Weibel ER.** Alterations of the gas exchange apparatus in adult respiratory insufficiency associated with septicemia. *Am Rev Respir Dis* 116: 589–615, 1977.
5. **Barazzone C, Horowitz S, Donati YR, Rodriguez I, and Piguet PF.** Oxygen toxicity in mouse lung: pathways to cell death. *Am J Respir Cell Mol Biol* 19: 573–581, 1998.
6. **Barazzone C, Donati YR, Rochat AF, Vesin C, Kan CD, Pache JC, and Piguet PF.** Keratinocyte growth factor protects alveolar epithelium and endothelium from oxygen-induced injury in mice. *Am J Pathol* 154: 1479–1487, 1999.
7. **Buckley S, Driscoll B, Anderson KD, and Warburton D.** Cell cycle in alveolar epithelial type II cells: integration of Matrigel and KGF. *Am J Physiol Lung Cell Mol Physiol* 273: L572–L580, 1997.
8. **Buckley S, Driscoll B, Anderson KD, and Warburton D.** Apoptosis and DNA damage in AEC2 cultured from hyperoxic rats. *Am J Physiol Lung Cell Mol Physiol* 274: L714–L720, 1998.
9. **Bui KC, Wu F, Buckley S, Wu LT, Williams R, Carbonaro-Hall D, Hall FL, and Warburton D.** Developmental and cell cycle dependent expression of cyclin A in alveolar epithelial cells. *Am J Respir Cell Mol Biol* 9: 115–125, 1993.
10. **Bui KC, Buckley S, Wu F, Uhal B, Joshi I, Liu J, Hussein M, Makhoul I, and Warburton D.** Induction of A- and D-type cyclins and cdc2 kinase activity during recovery from short term hyperoxic lung injury. *Am J Physiol Lung Cell Mol Physiol* 268: L262–L635, 1995.
11. **Corti M, Brody AR, and Harrison JH.** Isolation and primary culture of murine alveolar type II cells. *Am J Respir Cell Mol Biol* 14: 309–315, 1996.
12. **Driscoll B, Buckley S, Bui KC, Anderson KD, and Warburton D.** Telomerase in alveolar epithelial development and repair. *Am J Physiol Lung Cell Mol Physiol* 279: L1191–L1198, 2000.
13. **Evans MJ, Cabral LJ, Stevens RJ, and Freeman G.** Renewal of the terminal bronchiolar epithelium in the rat following exposure to NO_2. *Am J Pathol* 70: 175–190, 1973.
14. **Evans MJ, Cabral LJ, Stevens RJ, and Freeman G.** Transformation of alveolar type 2 cells to type 1 cells following exposure to NO2. *Exp Mol Pathol* 22: 142–150, 1975.
15. **Evans MJ and Kaufman MH.** Establishment in culture of pluripotential cells from mouse embryos. *Nature* 292: 154–156, 1981.
16. **Gorbunova V, Seluanov A, and Pereira-Smith OM.** Expression of human telomerase (hTERT) does not prevent stress-induced senescence in normal human fibroblasts but protects the cells from stress-induced apoptosis and necrosis. *J Biol Chem* 277: 38540–38549, 2002.
17. **Harris JB, Chang LY, and Crapo JD.** Rat lung alveolar type I epithelial cell injury and response to hyperoxia. *Am J Respir Cell Mol Biol* 4: 115–125, 1991.
18. **Hudak BB, Zhang LY, and Kleeberger SR.** Inter-strain variation in susceptibility to hyperoxic injury of murine airways. *Pharmacogenetics* 3: 135–143, 1993.
19. **Kroemer G and Reed JC.** Mitochondrial control of cell death. *Nat Med* 6: 513–519, 2000.
20. **Lane EB, Hogan BL, Kurkinen M, and Garrels JI.** Co-expression of vimentin and cytokeratins in parietal endoderm cells of early mouse embryo. *Nature* 303: 701–704, 1983.
21. **Lightfoot RT, Khov S, and Ischiropoulos H.** Transient injury to rat lung mitochondrial DNA after exposure to hyperoxia and inhaled nitric oxide. *Am J Physiol Lung Cell Mol Physiol* 286: L23–L29, 2004.
22. **McGrath SA.** Induction of p21WAF/CIP1 during hyperoxia. *Am J Respir Cell Mol Biol* 18: 179–187, 1998.
23. **McGrath-Morrow SA, Cho C, Soutiere S, Mitzner W, and Tuder R.** The effect of neonatal hyperoxia on the lung of p21Waf1/Cip1/Sdi1-deficient mice. *Am J Respir Cell Mol Biol* 30: 635–640, 2004.
24. **Miller BE and Hook GE.** Hypertrophy and hyperplasia of alveolar type II cells in response to silica and other pulmonary toxicants. *Environ Health Perspect* 85: 15–23, 1990.
25. **Morse D, Otterbein LE, Watkins S, Alber S, Zhou Z, Flavell RA, Davis RJ, and Choi AM.** Deficiency in the c-Jun NH_2-terminal kinase signaling pathway confers susceptibility to hyperoxic lung injury in mice. *Am J Physiol Lung Cell Mol Physiol* 285: L250–L257, 2003.
26. **O'Reilly MA, Staversky RJ, Stripp BR, and Finkelstein JN.** Exposure to hyperoxia induces p53 expression in mouse lung epithelium. *Am J Respir Cell Mol Biol* 18: 43–50, 1998.
27. **O'Reilly MA, Staversky RJ, Watkins RH, Maniscalco WM, and Keng PC.** p53-independent induction of GADD45 and GADD153 in mouse lungs exposed to hyperoxia. *Am J Physiol Lung Cell Mol Physiol* 278: L552–L559, 2000.
28. **O'Reilly MA.** DNA damage and cell cycle checkpoints in hyperoxic lung injury: braking to facilitate repair. *Am J Physiol Lung Cell Mol Physiol* 281: L291–L305, 2001.
29. **Pagano A and Barazzone-Argiroffo C.** Alveolar cell death in hyperoxia-induced lung injury. *Ann NY Acad Sci* 1010: 405–416, 2003.

30. **Perkowski S, Sun J, Singhal S, Santiago J, Leikauf GD, and Albelda SM.** Gene expression profiling of the early pulmonary response to hyperoxia in mice. *Am J Respir Cell Mol Biol* 28: 682–696, 2003.
31. **Reddy R, Buckley S, Doerken M, Barsky L, Weinberg K, Anderson KD, Warburton D, and Driscoll B.** Isolation of a putative progenitor subpopulation of alveolar epithelial type 2 cells. *Am J Physiol Lung Cell Mol Physiol* 286: L658–L667, 2004.
32. **Rice WR, Conkright JJ, Na CL, Ikegami M, Shannon JM, and Weaver TE.** Maintenance of the mouse type II cell phenotype in vitro. *Am J Physiol Lung Cell Mol Physiol* 283: L256–L264, 2002.
33. **Rinaldo JE and Rogers RM.** Adult respiratory-distress syndrome: changing concepts of lung injury and repair. *N Engl J Med* 306: 900–909, 1982.
34. **Roper JM, Mazzatti DJ, Watkins RH, Maniscalco WM, Keng PC, and O'Reilly MA.** In vivo exposure to hyperoxia induces DNA damage in a population of alveolar type II epithelial cells. *Am J Physiol Lung Cell Mol Physiol* 286: L1045–L1054, 2004.
35. **Staversky RJ, Watkins RH, Wright TW, Hernady E, LoMonaco MB, D'Angio CT, Williams JP, Maniscalco WM, and O'Reilly MA.** Normal remodeling of the oxygen-injured lung requires the cyclin-dependent kinase inhibitor p21(Cip1/WAF1/Sdi1). *Am J Pathol* 161: 1383–1393, 2002.
36. **Tryka AF, Witschi H, Gosslee DG, McArthur AH, and Clapp NK.** Patterns of cell proliferation during recovery from oxygen injury. *Am Rev Respir Dis* 133: 1055–1059, 1986.
37. **Ulich TR, Yi ES, Longmuir K, Yin S, Blitz R, Morris CF, Housley RM, and Pierce GF.** Keratinocyte growth factor is a growth factor for type II pneumocytes in vivo. *J Clin Invest* 93: 1298–1306, 1994.
38. **Waxman AB, Einarsson O, Seres T, Knickelbein RG, Warshaw JB, Johnston R, Homer RJ, and Elias JA.** Targeted lung expression of Interleukin-11 enhances murine tolerance of 100% oxygen and diminishes hyperoxia-induced DNA fragmentation. *J Clin Invest* 101: 1970–1982, 1998.
39. **Wu F, Buckley S, Bui KC, and Warburton D.** Differential expression of cyclin D2 and cdc2 genes in proliferating and nonproliferating alveolar epithelial cells. *Am J Respir Cell Mol Biol* 12: 95–103, 1995.